Title

Identify the nonlinear wave-particle interaction regime in rising tone chorus generation

Journal

Geophysical Research Letters, 44(8)

ISSN

0094-8276

Authors

Tao, Xin
Zonca, Fulvio
Chen, Liu

Publication Date

2017-04-28

DOI

10.1002/2017gl072624

AGU PUBLICATIONS

Geophysical Research Letters

RESEARCH LETTER
10.1002/2017GL072624

Key Points:
- Nonlinear wave-particle interaction is demonstrated to be nonadiabatic
- The nonlinear evolution timescale is comparable to the particle phase-space trapping timescale
- Subpacket formation is explained using phase-space bounce motion of particles

Correspondence to:
X. Tao,
xtao@ustc.edu.cn

Citation:
Tao, X., F. Zonca, and L. Chen (2017), Identify the nonlinear wave-particle interaction regime in rising tone chorus generation, *Geophys. Res. Lett.*, *44*, 3441–3446, doi:10.1002/2017GL072624.

Received 13 JAN 2017
Accepted 15 MAR 2017
Accepted article online 5 APR 2017
Published online 22 APR 2017

Identify the nonlinear wave-particle interaction regime in rising tone chorus generation

Xin Tao[1,2], Fulvio Zonca[3,4], and Liu Chen[4,5]

[1]CAS Key Laboratory of Geospace Environment, Department of Geophysics and Planetary SciencesUniversity of Science and Technology of China, Hefei, China, [2]Collaborative Innovation Center of Astronautical Science and Technology, Harbin, China, [3]ENEA C. R. Frascati, Frascati, Italy, [4]Institute of Fusion Theory and Simulation and Department of Physics, Zhejiang University, Hangzhou, China, [5]Department of Physics and Astronomy, University of California, Irvine, California, USA

Abstract Nonlinear wave-particle interaction during chorus wave generation was assumed to be in the adiabatic regime in previous studies, i.e., the particle phase-space trapping timescale (τ_{tr}) is considered to be much smaller than the nonlinear dynamics timescale τ_{NL}. In this work, we use particle-in-cell simulations to demonstrate that $\tau_{tr} \sim \tau_{NL}$, i.e., the interaction regime during chorus generation is in the nonadiabatic regime. The timescale for nonlinear evolution of resonant particle phase-space structures is determined by making the time-averaged power exchange plot, which clearly demonstrates that particles with pitch angle near 80° make the most significant contribution to wave growth. The phase-space trapping timescale is also comparable to the amplitude modulation timescale of chorus, suggesting that chorus subpackets are formed because of the self-consistent evolution of resonant particle phase-space structures and spatiotemporal features of the fluctuation spectrum.

1. Introduction

The physical mechanism of frequency chirping of chorus waves has been under debate for more than 50 years. Early theoretical models have identified the importance of nonlinear wave-particle interactions in frequency chirping [*Helliwell*, 1967; *Dysthe*, 1971; *Nunn*, 1974; *Vomvoridis et al.*, 1982; *Omura et al.*, 2008]. In a phenomenological model, *Helliwell* [1967] proposed the idea that the gyroresonance condition is maintained despite the background magnetic inhomogeneity; therefore, the coupling time between particles and the wave field is increased, leading to maximization of wave intensity. Although some aspects of the Helliwell model are debatable, the idea of particle phase trapping or phase locking has been widely adopted by later theoretical studies of frequency chirping in space plasmas [*Sudan and Ott*, 1971; *Nunn*, 1974; *Vomvoridis et al.*, 1982; *Omura et al.*, 2008]. Recent particle-in-cell simulations even directly observed the resulting phase-space structures by these phase-trapped particles [*Hikishima and Omura*, 2012].

Studies about frequency chirping of Alfvén waves in tokamak fusion devices have lead to theories for two different nonlinear wave-particle interaction regimes. Depending on particle phase-space trapping timescale (τ_{tr}) and the characteristic timescale of nonlinear evolution (τ_{NL}), the nonlinear wave-particle interaction can be categorized into the adiabatic regime and the nonadiabatic regime. In the adiabatic regime, $\tau_{NL} \gg \tau_{tr}$, leading to well-separated two timescales. An adiabatic invariant exists for the phase-space trapping motion. This adiabatic invariant typically is the action (J) corresponding to the phase-space bounce motion of trapped particles, i.e., $J = \oint p dq$, where p and q are canonical momentum and coordinates, respectively. A hole-clump model for frequency chirping has been proposed by *Berk et al.* [1997] for this regime, leading to the "bump-on-tail" paradigm of energetic particle driven Alfvén waves in tokamak fusion devices. In this regime, the system evolves slowly compared to the particle trapping timescale, and a perturbative analysis is used to investigate the evolution of the hole-clump structures. It was found that phase-space holes and clumps are formed simultaneously, and the frequency shifts so that the power taken from resonant particles is balanced by the background dissipation. On the other hand, if $\tau_{tr} \sim \tau_{NL}$, the interaction is nonadiabatic. An example is the "fishbone" paradigm for energetic particle-driven Alfvén waves in tokamaks [*Chen et al.*, 1984]. In this regime, the contribution to the wave dispersion relation is dominated by energetic particles. The wave-particle phase is locked, and the power transfer is maximized due to frequency chirping. A general theoretical framework for describing energetic particle distribution evolution in fusion plasmas has been

proposed by *Zonca et al.* [2015] and *Chen and Zonca* [2016]. To further understand the frequency chirping mechanism of chorus, it is important to identify the nonlinear wave-particle interaction regime, which is the main motivation of this study.

One key question in determining the nonlinear interaction regime is how to correctly estimate the phase-space trapping timescale. The nonrelativistic electromagnetic phase-space trapping frequency is $\omega_t = \sqrt{kv_\perp q\delta B/mc}$, where k is wave number, δB is the transverse wave magnetic field, q is the charge, m is the mass, and c is the speed of light in vacuum. Here the velocity perpendicular to the ambient background magnetic field, $v_\perp$, cannot be determined from cyclotron resonance condition alone. Some of previous studies used average perpendicular velocity of resonant particles in calculation of ω_t [*Ossakow et al.*, 1972; *Omura et al.*, 2008]. This way of calculating ω_t does not differentiate between contributions to the power transfer between particles with different $v_\perp$. In this work, we propose that the trapping frequency important to wave excitation can be determined by calculating the time-averaged power transfer from particles to the wave. As the lowest order approximation, the trapping timescale should be determined using the perpendicular velocity of particles maximizing power exchange with the wave. Note that when relativistic effects become important, the trapping frequency is $\omega_{tr} = \omega_t\delta\gamma^{-1/2}$, according to *Omura et al.* [2008] and *Tao and Bortnik* [2010]. Here $\gamma = (1 - v^2/c^2)^{-1/2}$ is the relativistic factor, and $\delta^2 = 1 - \omega^2/c^2k^2$, with ω the wave frequency. For our simulation below and typical conditions in the inner magnetosphere, $\delta \sim 1$; therefore, we use $\omega_{tr} \approx \omega_t\gamma^{-1/2}$ in this study.

As will be shown later in this work, a question closely related to the determination of the trapping timescale is the physical mechanism of the formation of chorus subpackets. The waveform of a chorus element typically shows quasi-periodic amplitude modulation, forming the so-called subpackets [*Santolík et al.*, 2003]. *Santolík et al.* [2003] suggested that the subpacket could be formed due to wave beating or it might be part of the inherent generation process. *Shoji and Omura* [2013] proposed that the subpacket is formed due to a sequential triggering process, where the nonlinear growth takes place over a limited time called nonlinear growth time. This process is repeated due to the generation of a new triggering wave by phase-organized particles. *Omura and Nunn* [2011] numerically determined that the this nonlinear growth time is on the same order as the particle phase-space trapping period. In this work, we suggest that the formation of chorus subpacket is directly due to phase-space bounce motion of electrons in the resonant island via a process described by *O'Neil* [1965], as will be discussed in detail in the text. This mechanism can naturally explain why the subpacket period is roughly the phase-space trapping period of particles, which will also be supported by our numerical simulations.

2. Numerical Simulation

In this work, we use the 1-D particle-in-cell simulation code, DAWN [*Tao*, 2014], to study chorus excitation. The DAWN code treats cold electrons as fluid and hot electrons using particle-in-cell technique, following the Electron Hybrid Model of *Katoh and Omura* [2007]. The background magnetic field is parabolic, $B = B_0(1 + \xi z^2)$, approximating the field near minimum B along a field line, which is believed to be the source region of chorus. Here z can be regarded as the distance along the field line from the equator, and B_0 is the field strength at equator. The inhomogeneity parameter $\xi = 4.5/(LR_p)^2$ for a dipole field, where L is the L shell and R_p is the planet radius. The distribution of hot electrons is bi-Maxwellian with perpendicular temperature larger than parallel temperature to drive whistler-mode waves. Note that only parallel propagating whistler waves are allowed in the DAWN code. Other details of the DAWN code can be found in *Tao* [2014]. For the simulation in this work, we choose $\xi = 8.62\times10^{-5}c^{-2}\Omega_{e0}^2$ and $\omega_{pe}/|\Omega_{e0}| = 5$. Here ω_{pe} is the cold electron plasma frequency, and Ω_{e0} is the signed electron cyclotron frequency at equator. For hot electrons, we choose parallel and perpendicular thermal velocities to be $0.2c$ and $0.53c$, respectively, and the density is 6% of cold electrons. Other technical simulation parameters are the same as those used by *Tao et al.* [2014].

Figure 1 presents the frequency-time spectrogram of simulated chorus element calculated using wave magnetic field normalized by B_0. Figure 1 (top) shows that the element starts from about $0.27|\Omega_{e0}|$ at $t \sim 1133|\Omega_{e0}|^{-1}$ and ends near $0.67|\Omega_{e0}|$ at $t \sim 1886|\Omega_{e0}|^{-1}$. The average frequency sweep rate is $\partial\omega/\partial t \sim 5.3 \times 10^{-4}|\Omega_{e0}|^2$. Figure 1 (bottom) demonstrates the waveform of the element from $t = 1050|\Omega_{e0}|^{-1}$ to t=1700$|\Omega_{e0}|^{-1}$, which clearly shows the quasi-periodic modulation of the wave amplitude and the resulting subpackets [*Santolík et al.*, 2003]. Black vertical dashed line denotes $t|\Omega_{e0}|$=1265, 1357, 1489, 1594, marking four identified subpackets. Period of these subpackets varies from roughly $92|\Omega_{e0}|^{-1}$ to $130|\Omega_{e0}^{-1}$. We will

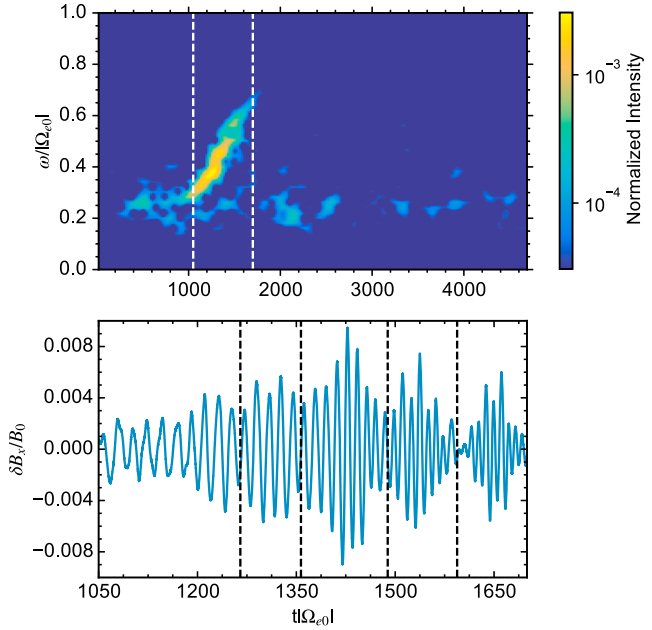

Figure 1. (top) Frequency-time spectrogram showing chorus element from the DAWN code simulation. Color coded is the normalized wave intensity. The two vertical dashed lines represent the time range during which the waveform of the element is plotted in Figure 1 (bottom). (bottom) Waveform plot from $t|\Omega_{e0}| = 1050$ to 1700. The boundaries of the selected subpackets are marked by four vertical dashed lines at $t|\Omega_{e0}| = 1265, 1357, 1489$, and 1594.

approximately use $T_{sp} \approx 110|\Omega_{e0}|^{-1}$, because we will only be interested in comparing the ordering of timescales.

3. Identification of the Nonlinear Wave-Particle Interaction Regime

To identify the nonlinear wave-particle interaction regime, we save 10 particle distributions from $t = 1000|\Omega_{e0}|^{-1}$ to $t=2500|\Omega_{e0}|^{-1}$. Two of these distributions at $t=1333|\Omega_{e0}|^{-1}$ and $1500|\Omega_{e0}|^{-1}$ are studied in detail in this work because they show the most identifiable nonlinear phase-space structures. Figure 2 demonstrates two kinds of histograms of particle distributions at two different times. Figure 2 (top row) shows the number of particles, or particle counts, per each $v_\perp - v_\parallel$ bin. Note that the number of particles per $v_\perp - v_\parallel$ bin is proportional to $fv_\perp$, where f is the phase-space density; therefore, if we divide this histogram by $v_\perp$, the resulting function will be proportional to f. Each count histogram shows a stripe of reduced particle counts along a curve, corresponding to the resonant curve of the generated wave frequency at these two different times. These histograms have been presented and discussed in previous studies [e.g., *Hikishima and Omura*, 2012]. However, it is hard to determine which group of particles can be used to calculate the trapping frequency $\omega_t = \sqrt{kv_\perp q\delta B/mc}$ or the relativistic version ω_{tr} from this kind of histogram, since $v_\perp$ cannot be determined from the cyclotron resonant condition alone.

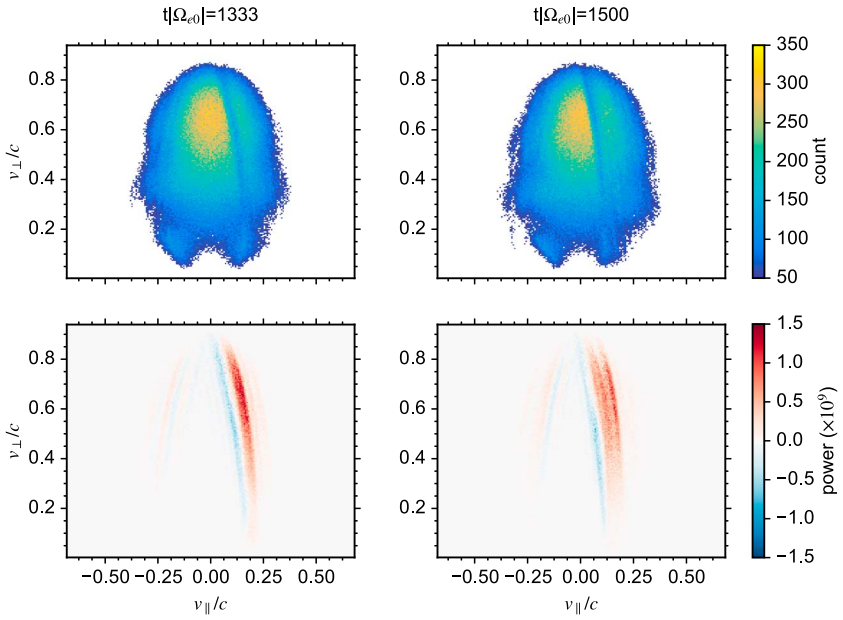

Figure 2. Two-dimensional histogram of (top row) count and (bottom row) time-averaged power transfer in $v_\perp - v_\parallel$ space at (left column) $t = 1333|\Omega_{e0}|^{-1}$ and (right column) $1500|\Omega_{e0}|^{-1}$.

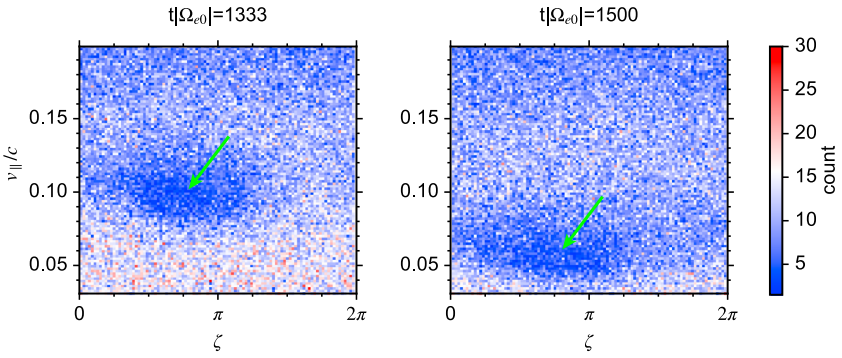

Figure 3. Histogram of count in $v_{\parallel} - \zeta$ phase space for a $v_{\perp} = 0.65c$ at equator at (left) $t = 1333|\Omega_{e0}|^{-1}$ and (right) $1500|\Omega_{e0}|^{-1}$. The two green arrows point to the center of the two phase-space holes.

To determine the appropriate $v_{\perp}$ used in the calculation of ω_{tr}, we make the time-averaged power transfer plot, shown in Figure 2 (bottom row). The time-averaged power transfer for the i_{th} simulation particle is

$$P_i = -\frac{1}{T}\left\langle q\boldsymbol{E}_i \cdot \boldsymbol{v}_i \right\rangle, \tag{1}$$

where $\langle \cdots \rangle = \int_t^{t+T} dt$ denotes time average, $\boldsymbol{E}$ is the electric field felt by the particle, and $\boldsymbol{v}$ is the velocity. The minus sign here is used so that if P_i is positive, the particle transfers energy to the wave, and vice versa. We use P_i as weight when calculating the power transfer histogram shown in Figure 2 (bottom row). The length of the average time window is $50|\Omega_{e0}|^{-1}$, which approximately equals half of the phase-space trapping period as will be discussed in detail below.

The power histogram plots in Figure 2 clearly demonstrate that resonant particles with $v_{\perp} \approx 0.65c$ transfer most energy to the wave; the corresponding pitch angle is about 80°. Figure 3 presents the count histograms in $v_{\parallel} - \zeta$ space for $v_{\perp} = 0.65c$ using particles around the equator, where ζ is the phase angle between $\boldsymbol{v}_{\perp}$ and wave magnetic field. Two phase-space holes can be clearly seen; these phase-space holes represent resonant islands [*Lichtenberg and Lieberman*, 1983] and are due to that the density of phase-trapped particles is lower than the surrounding untrapped particles [*Vomvoridis et al.*, 1982; *Omura et al.*, 2008; *Hikishima and Omura*, 2012]. Besides phase-trapped electrons, resonant but untrapped particles passing around the island shown in Figure 3 are phase-bunched particles. Phases of phase-bunched particles are confined to a narrow range when interacting with the wave, leading to a change in energy or pitch angle with roughly the same sign [*Albert*, 2000; *Bortnik et al.*, 2008; *Tao et al.*, 2012, 2013].

To calculate the trapping frequency, note that the $v_{\parallel}$ coordinate of the center of these phase-space holes denotes the resonant velocity v_R at the time corresponding to $v_{\perp} = 0.65c$. For $v_{\perp} = 0.65c$, $v_R \approx 0.11c$ at $t = t_0 \equiv 1333|\Omega_{e0}|^{-1}$ and $v_R \approx 0.06c$ at $t = t_1 \equiv 1500|\Omega_{e0}|^{-1}$. From the cyclotron resonance condition $\omega - kv_R = |\Omega_{e0}|/\gamma$, we determine that $\omega/|\Omega_{e0}| = 0.35$, $ck/|\Omega_{e0}| = -3.7$ for $t = t_0$ and $\omega/|\Omega_{e0}| = 0.47$, $ck/|\Omega_{e0}| = -4.8$ for $t = t_1$. The resonant frequencies are consistent with frequencies of the generated chorus element at these two times. The wave amplitude ($\delta B/B_0$) felt by particles is 1.6×10^{-3} for $t = t_0$ and 1.9×10^{-3} for $t = t_1$. The ordering of the amplitude is consistent with observations. The corresponding relativistic trapping frequency $\omega_{tr} \approx 0.059|\Omega_{e0}|$ and $0.062|\Omega_{e0}|$ at $t = t_0$ and t_1, respectively. The trapping period $T_{tr} \equiv 2\pi/\omega_{tr} \approx 106|\Omega_{e0}|^{-1}$ and $101|\Omega_{e0}|^{-1}$. Note that the average trapping period is about the same as the average subpacket period, $110|\Omega_e|^{-1}$, obtained in the previous section.

Now, it is crucial to compare the nonlinear evolution timescale and the trapping timescale. One way of comparing the two timescales is to compare the change of wave frequency within one trapping period with the trapping frequency itself. Using $\partial\omega/\partial t \approx 5.3 \times 10^{-4}|\Omega_{e0}|^2$ and $\omega_{tr} \approx 0.060|\Omega_{e0}|$, it is straightforward to show that

$$T_{tr}\frac{\partial\omega}{\partial t} \approx \omega_{tr}, \quad \text{or} \quad \frac{\partial\omega}{\partial t} \sim \frac{\omega_{tr}^2}{2\pi}. \tag{2}$$

An equivalent way is to calculate the change of resonant velocity within one trapping period and compare this with the resonant island half width. The variation of resonant velocity can be obtained by comparing the

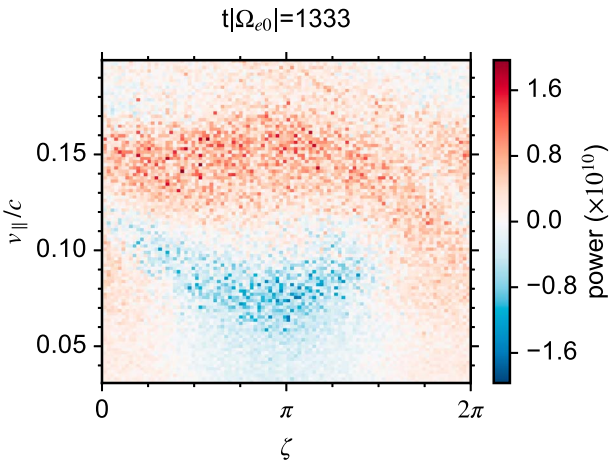

Figure 4. Histogram of time-averaged power transfer in $v_{\parallel} - \zeta$ phase space for $v_{\perp} = 0.65c$ at equator at $t = 1333|\Omega_{e0}|$. Color coded is the time-averaged power transfer multiplied by 10^{10}.

variation of resonant velocity v_R between t_0 and t_1 and using interpolation to obtain the variation of v_R during one trapping period as

$$\Delta v_R \equiv v_R(t_0 + T_{tr}) - v_R(t_0) \approx \frac{T_{tr}}{t_1 - t_0} \left| v_R(t_1) - v_R(t_0) \right|. \quad (3)$$

If we directly use the two v_R's with $v_{\perp} = 0.65c$ obtained from Figure 3, then $\Delta v_R \approx 0.032c$. On the other hand, the resonant island half width can be estimated as

$$\Delta v_{\parallel} \approx 2\omega_{tr}/|k|. \quad (4)$$

Using values of ω_{tr} and k at these two times, $\Delta v_{\parallel} \approx 0.032c$ at $t = t_0$ and 0.026 at $t = t_1$. Therefore, we conclude that the variation of v_R is on the same order as the resonant island half width. These calculations suggest that the nonlinear wave-particle interaction in chorus generation is nonadiabatic. The nonadiabatic nature of interaction indicates that resonant wave-particle interactions modify whistler waves nonperturbatively [*Chen and Zonca*, 2016], leading to the frequency chirping. However, further research is needed to prove more directly the nonperturbative nature of the interaction and is out of scope of the present study.

4. Physical Mechanism of Subpacket Formation

As we have pointed out in previous sections, the subpacket period is about the same as the phase-space trapping period. This can be understood using Figure 4, showing the time-averaged power transfer plot in $v_{\parallel} - \zeta$ space for $v_{\perp} = 0.65c$ at $t|\Omega_{e0}| = 1333$. Compared with Figure 3 (left), particles in the bottom part of the resonant island lose energy to the wave, while those in the top part gain energy. This is because $v_{\parallel}$ and energy of phase-trapped particles show quasi-periodic oscillations with a period of the trapping frequency [see, e.g., *Vomvoridis et al.*, 1982; *Omura et al.*, 2008; *Albert et al.*, 2012; *Tao et al.*, 2013]. Roughly speaking, because the length of the time average window is about $T_{tr}/2$, particles in the top part of the trapping island experienced an increase in $v_{\parallel}$, and therefore a decrease in energy, and vice versa. If the total energy lost is not the same as the total energy gained by the particles, there will be a net oscillation in the total energy of all trapped particles at the trapping frequency. Because of energy conservation, there will be an oscillation in wave energy or wave amplitude at roughly the trapping period. This process naturally explains the formation of chorus subpacket and that $T_{tr} \sim T_{sp}$, where T_{sp} is the subpacket period. Note that the physical process described here is essentially the same as the process causing amplitude modulation in the nonlinear stage of Landau damping before phase mixing flattens the distribution within the trapping region. The detailed theory for that process can be found in *O'Neil* [1965].

5. Summary

In this work, we used time-averaged power transfer calculation to determine that particles with pitch angle near 80° contribute most to chorus wave growth in the simulation. The correspondingly determined particle trapping period is demonstrated to be comparable to the subpacket period. We propose that the subpacket is formed directly due to the phase-space bounce motion of particles via the same process for the amplitude modulation in the nonlinear stage of Landau damping originally studied by *O'Neil* [1965]. We also demonstrated that the nonlinear evolution timescale is comparable to the trapping timescale, therefore, the nonlinear wave-particle interaction is nonadiabatic. Our studies suggest that further development of chorus excitation theory should carefully taken into consideration both the motion of phase-trapped particles and that the interaction is nonadiabatic.

Acknowledgments
We acknowledge support by National Science Foundation of China (grants 41631071, 41474142, and 41421063) and U.S. DoE grant. The data for this paper are available by contacting the corresponding author.

References

Albert, J. M. (2000), Gyroresonant interactions of radiation belt particles with a monochromatic electromagnetic wave, *J. Geophys. Res.*, *105*(A9), 21,191–21,209.

Albert, J. M., X. Tao, and J. Bortnik (2012), Aspects of nonlinear wave-particle interactions, in *Dynamics of the Earth's Radiation Belts and Inner Magnetosphere, Geophys. Monogr. Ser.*, vol. 199, edited by D. Summers et al., pp. 255–264, AGU, Washington, D. C., doi:10.1029/2012GM001324.

Berk, H. L., B. N. Breizman, and N. V. Petviashvili (1997), Spontaneous hole-clump pair creation in weakly unstable plasmas, *Phys. Lett. A*, *234*(3), 213–218, doi:10.1016/S0375-9601(97)00523-9.

Bortnik, J., R. M. Thorne, and U. S. Inan (2008), Nonlinear interaction of energetic electrons with large amplitude chorus, *Geophys. Res. Lett.*, *35*, L21102, doi:10.1029/2008GL035500.

Chen, L., and F. Zonca (2016), Physics of Alfvén waves and energetic particles in burning plasmas, *Rev. Mod. Phys.*, *88*, 015008, doi:10.1103/RevModPhys.88.015008.

Chen, L., R. B. White, and M. N. Rosenbluth (1984), Excitation of internal kink modes by trapped energetic beam ions, *Phys. Rev. Lett.*, *52*(13), 1122–1125, doi:10.1103/PhysRevLett.52.1122.

Dysthe, K. B. (1971), Some studies of triggered whistler emissions, *J. Geophys. Res.*, *76*(28), 6915–6931.

Helliwell, R. A. (1967), A theory of discrete VLF emissions from the magnetosphere, *J. Geophys. Res.*, *72*(19), 4773–4790.

Hikishima, M., and Y. Omura (2012), Particle simulations of whistler-mode rising-tone emissions triggered by waves with different amplitudes, *J. Geophys. Res.*, *117*, A04226, doi:10.1029/2011JA017428.

Katoh, Y., and Y. Omura (2007), Computer simulation of chorus wave generation in the Earth's inner magnetosphere, *Geophys. Res. Lett.*, *34*, L03102, doi:10.1029/2006GL028594.

Lichtenberg, A., and M. Lieberman (1983), *Regular and Chaotic Dynamics*, 2nd ed., Springer, New York.

Nunn, D. (1974), A self-consistent theory of triggered VLF emissions, *Planet. Space Sci.*, *22*(3), 349–378, doi:10.1016/0032-0633(74)90070-1.

Omura, Y., and D. Nunn (2011), Triggering process of whistler mode chorus emissions in the magnetosphere, *J. Geophys. Res.*, *116*, A05205, doi:10.1029/2010JA016280.

Omura, Y., Y. Katoh, and D. Summers (2008), Theory and simulation of the generation of whistler-mode chorus, *J. Geophys. Res.*, *113*, A04223, doi:10.1029/2007JA012622.

O'Neil, T. (1965), Collisionless damping of nonlinear plasma oscillations, *Phys. Fluids*, *8*, 2255–2262, doi:10.1063/1.1761193.

Ossakow, S. L., E. Ott, and I. Haber (1972), Nonlinear evolution of whistler instabilities, *Phys. Fluids*, *15*(12), 2314–2326, doi:10.1063/1.1693875.

Santolík, O., D. A. Gurnett, J. S. Pickett, M. Parrot, and N. Cornilleau-Wehrlin (2003), Spatio-temporal structure of storm-time chorus, *J. Geophys. Res.*, *108*(A7), 1278, doi:10.1029/2002JA009791.

Shoji, M., and Y. Omura (2013), Triggering process of electromagnetic ion cyclotron rising tone emissions in the inner magnetosphere, *J. Geophys. Res. Space Physics*, *118*, 5553–5561, doi:10.1002/jgra.50523.

Sudan, R. N., and E. Ott (1971), Theory of triggered VLF emissions, *J. Geophys. Res.*, *76*(19), 4463–4476, doi:10.1029/JA076i019p04463.

Tao, X. (2014), A numerical study of chorus generation and the related variation of wave intensity using the DAWN code, *J. Geophys. Res. Space Physics*, *119*, 3362–3372, doi:10.1002/2014JA019820.

Tao, X., and J. Bortnik (2010), Nonlinear interactions between relativistic radiation belt electrons and oblique whistler mode waves, *Nonlinear Processes Geophys.*, *17*, 599–604, doi:10.5194/npg-17-599-2010.

Tao, X., J. Bortnik, R. M. Thorne, J. Albert, and W. Li (2012), Effects of amplitude modulation on nonlinear interactions between electrons and chorus waves, *Geophys. Res. Lett.*, *39*, L06102, doi:10.1029/2012GL051202.

Tao, X., J. Bortnik, J. M. Albert, R. M. Thorne, and W. Li (2013), The importance of amplitude modulation in nonlinear interactions between electrons and large amplitude whistler waves, *J. Atmos. Sol. Terr. Phys.*, *99*, 67–72, doi:10.1016/j.jastp.2012.05.012.

Tao, X., Q. Lu, S. Wang, and L. Dai (2014), Effects of magnetic field configuration on the day-night asymmetry of chorus occurrence rate: A numerical study, *Geophys. Res. Lett.*, *41*, 6577–6582, doi:10.1002/2014GL061493.

Vomvoridis, J. L., T. L. Crystal, and J. Denavit (1982), Theory and computer simulations of magnetospheric very low frequency emissions, *J. Geophys. Res.*, *87*(A3), 1473–1489, doi:10.1029/JA087iA03p01473.

Zonca, F., L. Chen, S. Briguglio, G. Fogaccia, G. Vlad, and X. Wang (2015), Nonlinear dynamics of phase space zonal structures and energetic particle physics in fusion plasmas, *New J. Phys.*, *17*(1), 031052, doi:10.1088/1367-2630/17/1/013052.